

Enzymes

The Crystal Structure of a Homodimeric *Pseudomonas* Glyoxalase I Enzyme Reveals Asymmetric Metallation Commensurate with Half-of-Sites ActivityRohan Bythell-Douglas,^[a] Uthaiwan Suttisansanee,^[b] Gavin R. Flematti,^[a] Michael Challenor,^[a] Mihwa Lee,^[a] Santosh Panjikar,^[c, d] John F. Honek,^[b] and Charles S. Bond^{*[a]}

Abstract: The Zn inactive class of glyoxalase I (Glo1) metalloenzymes are typically homodimeric with two metal-dependent active sites. While the two active sites share identical amino acid composition, this class of enzyme is optimally active with only one metal per homodimer. We have determined the X-ray crystal structure of GloA2, a Zn inactive Glo1 enzyme from *Pseudomonas aeruginosa*. The presented structures exhibit an unprecedented metal-binding arrangement consistent with half-of-sites activity: one active site contains a single activating Ni²⁺ ion, whereas the other contains two inactivating Zn²⁺ ions. Enzymological experiments prompted by the binuclear Zn²⁺ site identified a novel catalytic property of GloA2. The enzyme can function as a Zn²⁺/Co²⁺-dependent hydrolase, in addition to its previously determined glyoxalase I activity. The presented findings demonstrate that GloA2 can accommodate two distinct metal-binding arrangements simultaneously, each of which catalyzes a different reaction.

Half-of-sites activity is a phenomenon where only one of two essentially identical active sites of an enzyme is functional at any one time.^[1] This type of mechanism seems wasteful, as though cellular resources are spent producing an effectively nonfunctioning active site. A case-in-point is the Zn inactive glyoxalase I (Glo1) class of enzyme.

Glo1 is a metalloenzyme involved in the methylglyoxal detoxification system^[2] (Figure S1, Supporting Information). Struc-

tural studies have shown that Glo1 enzymes are typically homodimeric, with two identical metal-binding active sites related to one another by two-fold rotational symmetry.^[3] Glo1 enzymes can be categorized into Zn active and Zn inactive classes^[1b,4] (Figure S2, Supporting Information). Both classes require octahedral coordination of the active site metal for their canonical lyase activity, converting methylglyoxal-glutathione hemithioacetal to *S*-D-lactoylglutathione.^[5] Zn inactive Glo1 enzymes are inactive with Zn²⁺ bound, and are optimally active with Ni²⁺ bound.^[1b,4] These enzymes demonstrate half-of-sites activity, with optimal activity at a ratio of one metal ion per homodimer.^[1b,4] Furthermore, isothermal titration calorimetry and ¹⁵N-¹H HSQC NMR spectroscopic studies on the Zn inactive *Escherichia coli* Glo1 demonstrated asymmetry in metal-binding affinity.^[6] Despite these results, the crystal structure of the Zn inactive Glo1 enzyme from *E. coli* possesses full occupancy Ni²⁺ ions at each of the two active sites.^[3a] All published Zn inactive Glo1 structures are essentially symmetrical, providing no structural insight into half-of-sites activity.^[3a,7]

We present the first conspicuously asymmetric Zn inactive Glo1 crystal structure, GloA2 from *P. aeruginosa*. The enzyme possesses a single octahedrally coordinated Ni²⁺ at one active site and two Zn²⁺ ions at the other site, congruent with half-of-sites activity. We also present a novel hydrolytic function of GloA2, related to this metal-binding arrangement. These data suggest that GloA2 is capable of simultaneously possessing two completely different and catalytically active metal-binding arrangements, addressing the biological economy of this enzyme.

In all four presented structures, the two monomers that form the GloA2 homodimer are related to one another by noncrystallographic symmetry, as in other Glo1 enzyme structures^[3a,b,d,7] (Figure 1). The overall fold of GloA2 is almost identical to the *E. coli* Glo1 enzyme^[3a] (RMSD 0.39 Å for all 117 C α atoms for chain A and 0.93 for chain B (114/117)) (Table S2, Supporting Information) sharing the $\beta\alpha\beta\beta$ architecture.

The structures confirmed active metal-binding residues His5, Glu56, His74*, and Glu122*,^[8] in which asterisks denote the other chain of the homodimer. Metal ions were unambiguously identified by using anomalous difference density maps generated from diffraction data sets collected below and above the Ni and Zn X-ray absorption edges (Table S3, Supporting Information).

The electron density in all models was consistent with at least one full-occupancy metal ion at both of the metal-binding active sites (Figure 2). Structures were determined with

[a] Dr. R. Bythell-Douglas, Dr. G. R. Flematti, M. Challenor, Dr. M. Lee, Prof. C. S. Bond
School of Chemistry and Biochemistry, The University of Western Australia
35 Stirling Highway, Crawley 6009, Western Australia (Australia)
E-mail: charles.bond@uwa.edu.au

[b] Dr. U. Suttisansanee, Prof. J. F. Honek
Department of Chemistry, University of Waterloo
200 University Avenue West, Waterloo, Ontario, N2L 3G1 (Canada)

[c] Dr. S. Panjikar
Department of Biochemistry and Molecular Biology, Monash University
Clayton Campus, Melbourne 3800, Victoria (Australia)

[d] Dr. S. Panjikar
Australian Synchrotron, 800 Blackburn Road, Clayton
Victoria 3168 (Australia)

Supporting information for this article is available on the WWW under <http://dx.doi.org/10.1002/chem.201405402>.

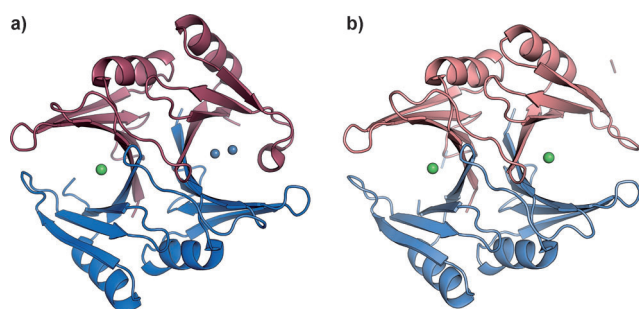


Figure 1. GloA2 (NiZn-GloA2.a; left) and Ni²⁺ bound *E. coli* Glo1^[3a] (right). Chain A is colored blue and chain B is colored red. Ni²⁺ and Zn²⁺ ions are shown as green and grey spheres.

a single Ni²⁺ at both sites (Ni–GloA2, 2.17 Å) and a single Zn²⁺ at both sites (Zn–GloA2, 1.83 Å). Two further structures were determined with a novel asymmetric metal-binding arrangement, with a Ni²⁺ ion at one site and two Zn²⁺ ions at the second site (Figure 3); one structure at high resolution (NiZn–GloA2.a, 1.80 Å) and the other with accompanying anomalous difference maps for metal identification (NiZn–GloA2.b, 2.17 Å). The additional Zn²⁺ is bound adjacent to the predicted position. As far as we are aware, this is the first time that a homodimeric metal-binding enzyme has been observed to bind a different metal at each active site. In these structures, residues Ala100 to Val109 (Loop-8) also demonstrate asymmetry. One monomer adopts a “folded in” conformation, orienting His105 appropriately to form the novel metal-binding site along with Glu122 (Figure S3, Supporting Information). Loop-8 on the other chain adopts a similar conformation to the *E. coli* Glo1 structure.

The coordination geometry of the active-site metals (Figure 4) provides insight into half-of-sites activity. The Ni²⁺

ion in NiZn-GloA2.a and NiZn-GloA2.b is bound in octahedral coordination geometry, appropriate for Glo1 activity. GloA2 has no Glo1 activity with Zn²⁺ bound^[8] hence the Zn²⁺-bound site is inactive.

The binuclear Zn site is a novel metal-binding arrangement for a Glo1 enzyme, and as such the role of this site was initially unclear. The two Zn²⁺ ions are 3.2 and 3.3 Å apart in structures NiZn-GloA2.a and NiZn-GloA2.b, respectively. These ions coordinate a bridging water molecule, an arrangement typical of a metallohydrolase.^[10] The second reaction of the methylglyoxal detoxification pathway is the hydrolysis of *S*-D-lactoylglutathione by the unrelated binuclear metallohydrolase Glo2.^[11] Based on the binuclear metal arrangement in the X-ray crystal structure, we generated the hypothesis that GloA2 can act as a Glo2.

Classical Glo1 and Glo2 enzymes are structurally unrelated^[11c,12] (Figure S6, Supporting Information). However, superimposing GloA2 and Glo2 structures by the coordinates of the binuclear metal centers demonstrates that the solvent accessibility and substrate-binding site of GloA2 is similar to Glo2 enzymes (Figure S7, Supporting Information).

Using HPLC-MS and established Glo2 kinetic protocols,^[12a] we determined that GloA2 consumes *S*-D-lactoylglutathione to produce lactate and glutathione, the products of the Glo2 reaction (Figure 5, Figure S8, Supporting Information). GloA2 has a *K_m* for the Glo2 reaction of 260 ± 27 μM (Figure S9, Supporting Information), similar to other characterized Glo2 enzymes.^[11b,12a,13] However, GloA2s *V_{max}* of 55 ± 3 nmol min⁻¹ mg⁻¹, *k_{cat}* of 0.027 s⁻¹ and *k_{cat}*/*K_m* of 100 M⁻¹ s⁻¹ are all three orders of magnitude lower than established Glo2 enzymes.^[11b,12a,13]

As the novel metal-binding site is comprised of His105 and Glu122, we generated the variants H105A and E122Q by site-directed mutagenesis to determine the influence of these resi-

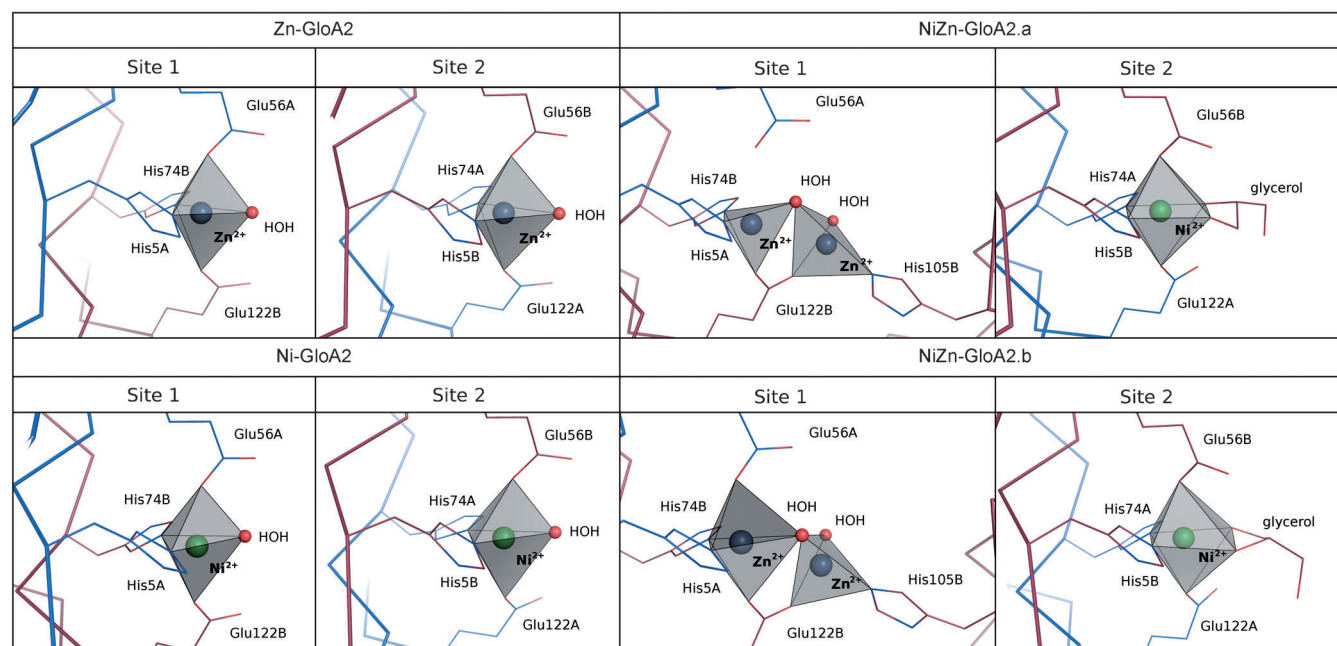


Figure 2. The coordination geometry of each active site metal is shown as a gray polyhedron. Lines between carbon atoms from chains A and B are colored blue and red, respectively. Zn²⁺ ions, Ni²⁺ ions and water-molecule oxygen atoms are colored as grey, green, and red spheres, respectively.

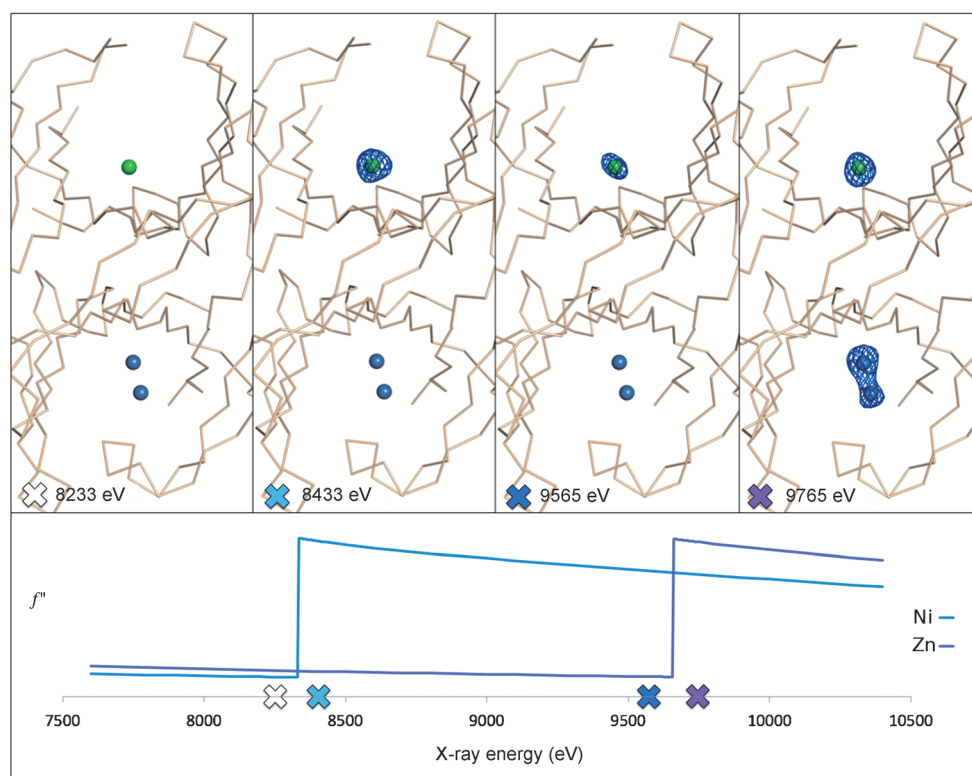


Figure 3. Anomalous difference electron-density maps of NiZn-GloA2.b collected at X-ray energies either side of the Ni and Zn X-ray absorption edges. NiZn-GloA2.b is shown as a ribbon with the metals shown as spheres. Dark blue mesh represents anomalous difference density (contoured at 3.5σ) for data collected at 8233, 8433, 9565, and 9765 eV. The bottom panel relates X-ray energy to the theoretical anomalous signal strength f'' of Ni and Zn^[9].

dues on GloA2 hydrolytic activity. Similar kinetic data were observed for H105A as the wild type, whereas the E122Q variant showed a significant decrease in activity relative to the wild type (K_m $780 \pm 880 \mu\text{M}$, V_{max} $6.9 \pm 5.6 \text{ nmol min}^{-1} \text{ mg}^{-1}$; Figure 6).

ICP-MS analysis of GloA2 demonstrated that Zn is the major metal species bound to the enzyme as isolated and purified from the *E. coli* expression host (Table S6, Supporting Information). Treating GloA2 with the chelating agent dipicolinic acid (DPA) resulted in a 66% decrease in Glo2 enzyme activity, confirming that GloA2 Glo2 activity is metal dependent (Figure 6). ICP-MS analysis of GloA2 incubated with excess ZnCl_2 demonstrated that the enzyme can bind three metal ions per homodimer in solution, validating the metal-binding stoichiometry observed in the crystal structure.

To identify the optimal Glo2 activity metal for GloA2, Glo2 activity was measured for protein spiked with a range of metal cations. Only Co^{2+} stimulated Glo2 activity (Figure 6). Attempts to use Zn^{2+} to metallate Apo-GloA2, however, resulted in inactive protein. The same effect has been observed previously in other binuclear Zn^{2+} active Glo2 enzymes^[11a,b] and has been attributed to mis-metallation.

We have determined the first crystal structure of a Zn inactive Glo1 enzyme that provides insight into half-of-sites activity. One of the two active sites is bound to Ni^{2+} in a configuration appropriate for Glo1 activity. The other site is bound to

Zn^{2+} , a metal ion that GloA2 cannot use to catalyze the Glo1 reaction. These data demonstrate that despite identical amino acid composition for each substrate-binding site, GloA2 is capable of an asymmetric metal-binding arrangement.

While Loop-8 provides His105 to coordinate the novel metal binding site (Figure S3, Supporting Information), there is no significant difference between wild-type and H105A variant GloA2 enzymes in terms of Glo2 enzyme kinetics. This result demonstrates that His105 is not essential for Glo2 activity. Our results do not delineate whether GloA2 requires a binuclear or mononuclear Zn^{2+} site for hydrolytic activity.

The slow rate at which GloA2 catalyzes the Glo2 reaction suggests that this capability is not likely physiologically relevant, as *P. aeruginosa* possesses a canon-

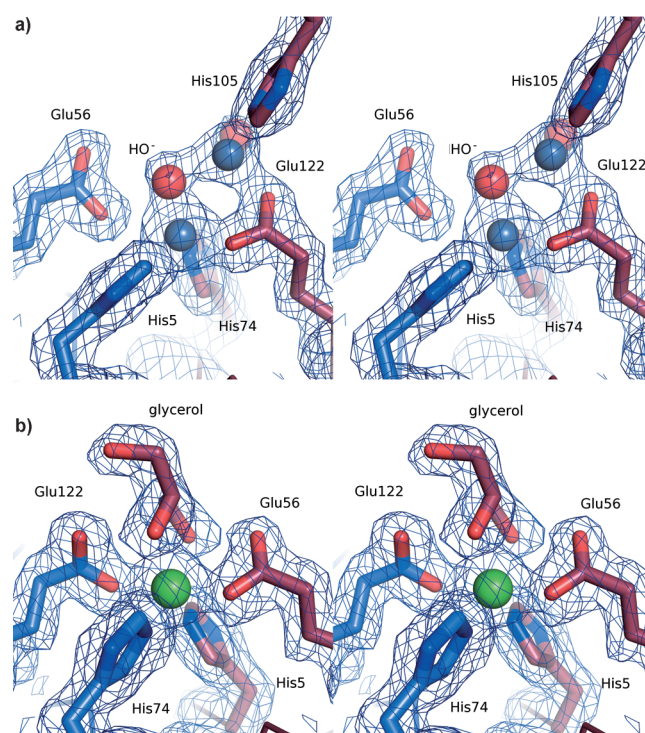


Figure 4. Stereoview of the two metal-bound active sites of NiZn-GloA2.a. a) The binuclear Zn bound active site. b) The Ni bound active site. Chains A and B are colored blue and red, respectively. Metal-binding residues and glycerol are shown in stick representation. Zn^{2+} and Ni^{2+} ions are shown in grey and green. Waters are shown as red spheres. $2m|F_o - D|F_c|$, electron-density maps (dark-blue mesh) are contoured to 1.0σ .

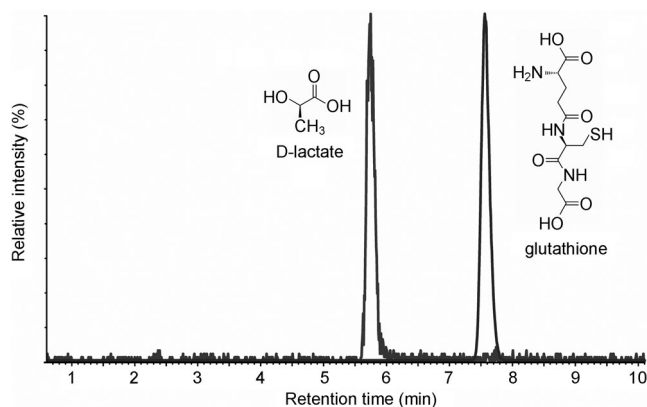


Figure 5. Extracted ion chromatograms of D-lactate ($[M-H]^-$ m/z : 89) and glutathione ($[M-H]^-$ m/z : 306) from a sample of GloA2 incubated with S-D-lactoylglutathione.

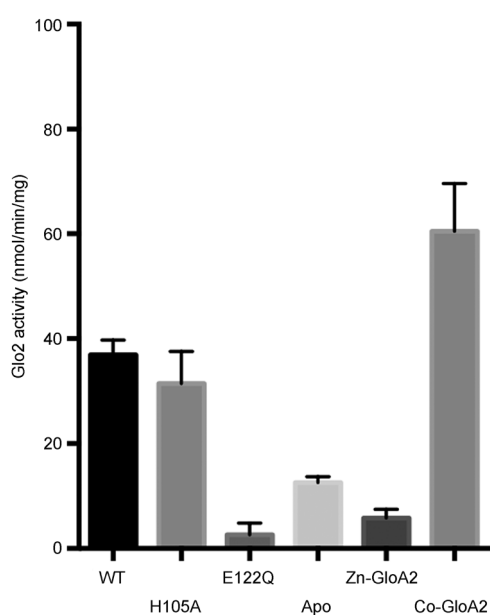


Figure 6. Glo2 activity of GloA2. WT: wild-type, H105A: H105A variant, E122Q: E122Q variant. Apo: DPA treated GloA2, Zn-GloA2: Zn^{2+} supplemented Apo-GloA2, Co-GloA2: Co^{2+} supplemented Apo-GloA2. Values correspond to the mean and standard error for three replicates.

cal Glo2 coding sequence (NCBI accession number; Q9I2T1).^[14] One explanation for this slow catalytic rate is that S-D-lactoylglutathione is not the true substrate for the hydrolytic activity of GloA2. Nonetheless, the kinetic data presented here clearly demonstrate that GloA2 can perform a Zn^{2+}/Co^{2+} dependent hydrolysis reaction. Collectively, the data presented here suggest that the half-of-sites activity of GloA2, and possibly other Zn inactive Glo1 enzymes, is related to alternate metal-binding functionalities of the second active site.

It is of particular note that GloA2 can catalyze two completely different reactions using the same underlying protein scaffold merely by switching the bound metal species. These results are especially interesting given the recent suggestion, based on studies of the *Plasmodium falciparum* Glo1, that the second active site of this enzyme may be optimized for either alternate substrates or regulatory molecules.^[15] These findings

provide novel insight in to the functional flexibility of metalloenzymes.

Acknowledgements

We acknowledge the use of beamlines MX1 and MX2 of the Australian Synchrotron, funded by the Western Australian Foundation Investor consortium. We thank the undergraduate students of UWA's CHEM3307 for participating in X-ray data collection. We thank Agata Sadowska, Denise Lupton and Paul Kirkwood for technical assistance. J.H. gratefully acknowledges the financial support of NSERC (Canada). U.S. gratefully acknowledges the financial support of the University of Waterloo (Ontario, Canada) and the Government of Thailand.

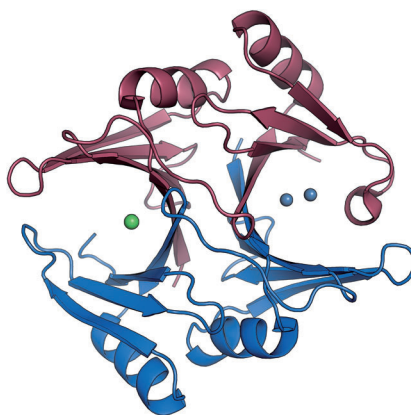
Keywords: crystal-structure determination · enzymes · metalloenzymes · proteins · zinc

- [1] a) J. F. Biellmann, P. Eid, C. Hirth, H. Jornvall, *Eur J Biochem* **1980**, *104*, 59–64; b) S. L. Clugston, J. F. Barnard, R. Kinach, D. Miedema, R. Ruman, E. Daub, J. F. Honek, *Biochemistry* **1998**, *37*, 8754–8763; c) S. I. Hauenstein, Y. M. Hou, J. J. Perona, *J Biol Chem* **2008**, *283*, 21997–22006; d) M. Sun, T. S. Leyh, *Biochemistry* **2010**, *49*, 4779–4785.
- [2] M. Sousa Silva, R. A. Gomes, A. E. Ferreira, A. Ponces Freire, C. Cordeiro, *Biochem. J.* **2013**, *453*, 1–15.
- [3] a) M. M. He, S. L. Clugston, J. F. Honek, B. W. Matthews, *Biochemistry* **2000**, *39*, 8719–8727; b) A. D. Cameron, B. Olin, M. Ridderstrom, B. Mannervik, T. A. Jones, *EMBO J.* **1997**, *16*, 3386–3395; c) A. Ariza, T. J. Vickers, N. Greig, A. H. Fairlamb, C. S. Bond, *Acta Crystallogr. Sect. F* **2005**, *61*, 769–772; d) M. Kawatani, *Proc. Natl. Acad. Sci. USA* **2008**, *105*, 11691–11696.
- [4] N. Sukdeo, S. L. Clugston, E. Daub, J. F. Honek, *Biochem. J.* **2004**, *384*, 111–117.
- [5] a) E. Racker, *J. Biol. Chem.* **1951**, *190*, 685–696; b) F. Himo, P. E. Siegbahn, *J. Am. Chem. Soc.* **2001**, *123*, 10280–10289.
- [6] a) S. L. Clugston, R. Yajima, J. F. Honek, *Biochem. J.* **2004**, *377*, 309–316; b) Z. Su, N. Sukdeo, J. F. Honek, *Biochemistry* **2008**, *47*, 13232–13241.
- [7] A. Ariza, T. J. Vickers, N. Greig, K. A. Armour, M. J. Dixon, I. M. Eggleston, A. H. Fairlamb, C. S. Bond, *Mol. Microbiol.* **2006**, *59*, 1239–1248.
- [8] N. Sukdeo, J. F. Honek, *Biochim. Biophys. Acta Proteins Proteomics* **2007**, *1774*, 756–763.
- [9] S. Brennan, P. L. Cowan, *Rev. Sci. Instrum.* **1992**, *63*, 850–853.
- [10] G. Schenk, N. Mitic, L. R. Gahan, D. L. Ollis, R. P. McGeary, L. W. Guddat, *Acc. Chem. Res.* **2012**, *45*, 1593–1603.
- [11] a) M. W. Crowder, M. K. Maiti, L. Banovic, C. A. Makaroff, *FEBS Lett.* **1997**, *418*, 351–354; b) J. O'Young, N. Sukdeo, J. F. Honek, *Arch. Biochem. Biophys.* **2007**, *459*, 20–26; c) A. D. Cameron, M. Ridderstrom, B. Olin, B. Mannervik, *Structure* **1999**, *7*, 1067–1078.
- [12] a) G. P. Marasinghe, I. M. Sander, B. Bennett, G. Periyannan, K. W. Yang, C. A. Makaroff, M. W. Crowder, *J. Biol. Chem.* **2005**, *280*, 40668–40675; b) M. S. Silva, L. Barata, A. E. Ferreira, S. Romao, A. M. Tomas, A. P. Freire, C. Cordeiro, *Biochemistry* **2008**, *47*, 195–204; c) V. A. Campos-Bermudez, N. R. Leite, R. Krog, A. J. Costa-Filho, F. C. Soncini, G. Oliva, A. J. Vila, *Biochemistry* **2007**, *46*, 11069–11079.
- [13] a) M. Akoachere, R. lozef, S. Rahlfs, M. Deponte, B. Mannervik, D. J. Creighton, H. Schirmer, K. Becker, *Biol. Chem.* **2005**, *386*, 41–52; b) M. Ridderstrom, B. Mannervik, *Biochem. J.* **1997**, *322* (Pt 2), 449–454.
- [14] C. K. Stover, *Nature* **2000**, *406*, 959–964.
- [15] M. Urscher, R. Alisch, M. Deponte, *Semin. Cell Dev. Biol.* **2011**, *22*, 262–270.

Received: September 25, 2014
Published online on ■■■, 0000

COMMUNICATION

Half-of-sites activity is a puzzling phenomenon where only one of two essentially identical active sites of an enzyme is catalytically active. Structural and kinetic studies on the metalloenzyme GloA2 demonstrated that the two sites are capable of adopting two completely different metal-binding arrangements, which catalyze two different reactions (see figure).



Enzymes

*R. Bythell-Douglas, U. Suttisansanee, G. R. Flematti, M. Challenor, M. Lee, S. Panjikar, J. F. Honek, C. S. Bond**



The Crystal Structure of a Homodimeric *Pseudomonas* Glyoxalase I Enzyme Reveals Asymmetric Metallation Commensurate with Half-of-Sites Activity

